doi: 10.12029/gc20200413

朱清波, 靳国栋, 赵希林, 张传林, 舒徐洁, 洪文涛. 2020. 赣北晚中生代岭上超镁铁岩的岩石成因：年代学与地球化学制约[J]. 中国地质, 47(4): 1092−1108.

Zhu Qingbo, Jin Guodong, Zhao Xilin, Zhang Chuanlin, Shu Xujie, Hong Wentao. 2020. Petrogenesis of the late Mesozoic Lingshang ultramafic intrusion in northern Jiangxi Province: Chronologic and geochemical constraints[J]. Geology in China, 47(4):1092−1108(in Chinese with English abstract).

赣北晚中生代岭上超镁铁岩的岩石成因：年代学与地球化学制约

朱清波[1],靳国栋[1],赵希林[1],张传林[2],舒徐洁[1],洪文涛[1,3]

(1. 中国地质调查局南京地质调查中心, 江苏 南京 210016; 2. 河海大学,江苏 南京 210098; 3. 南京大学,江苏 南京 210023)

提要：华南内陆在晚中生代发生了广泛的岩石圈伸展减薄事件，赣北新余地区的岭上超镁铁岩体形成于(120.8±1.4) Ma的早白垩世晚期，其作为钦杭结合带东段早白垩世幔源岩浆活动的记录，是研究华南中部晚中生代地幔属性及地球深部动力学过程的良好对象。在系统分析岭上超镁铁质岩的LA−MC−ICP−MS锆石U−Pb年代学、Lu−Hf同位素和元素地球化学特征的基础上，探讨了该超镁铁质岩的源区特征及其所反映的大地构造背景。数据表明，岭上超镁铁岩在形成过程中未遭受明显的地壳混染，其MgO含量集中且与TiO_2、Al_2O_3、Ni、Th等元素之间不存在明显的线性关系，反映该岩体未发生显著的结晶分异作用。但$Mg^{\#}$的变化范围和La−Sm分异程度反映堆晶作用和部分熔融可能对岩浆演化有所影响。稀土和微量元素(如Nb、Ta 、Zr、Hf等)特征类似于板内玄武岩(OIB)，低SiO_2、高Ti、高Fe/Mn比值和Ni等特征均显示与软流圈地幔关系密切。但锆石$\varepsilon_{Hf}(t)$(6.83~11.41)未达到亏损地幔的程度、Nb/Ta比值接近于岩石圈地幔值，且在相关元素图解中具尖晶石橄榄岩地幔源区低程度部分熔融的特征。反映岭上超镁铁岩可能是晚中生代陆内伸展背景下，上涌的软流圈物质与富集岩石圈地幔相互作用并发生部分熔融，深部超镁铁质岩浆沿构造薄弱带快速侵位的产物。

关　键　词：超镁铁岩；晚中生代；岩石圈伸展减薄；OIB；地质调查工程；江西

中图分类号：P597⁺.3 ;P595　　**文献标志码**：A　　**文章编号**：1000−3657(2020)04−1092−17

Petrogenesis of the late Mesozoic Lingshang ultramafic intrusion in northern Jiangxi Province: Chronologic and geochemical constraints

ZHU Qingbo[1], JIN Guodong[1], ZHAO Xilin[1], ZHANG Chuanlin[2], SHU Xujie[1], HONG Wentao[1,3]

(1. *China Geological Survey Nanjing Geological Survey Center, Nanjing* 210016*, Jiangsu, China;* 2. *Hohai University, Nanjing* 210016, *Jiangsu, China;* 3. *Nanjing University, Nanjing* 210023*, Jiangsu, China)*

Abstract: Extensive lithospheric extensional thinning events occurred during the late Mesozoic in the interior of South China block. As a record of the early Cretaceous ((120.8±1.4)Ma) mantle−derived magmatic activities in the eastern part of the Qingzhou—Hangzhou juncture belt, the Lingshang ultramafic intrusion in Xinyu of northern Jiangxi is a good object for studying the mantle

收稿日期：2019−04−29；**改回日期**：2020−04−19

基金项目：中国地质调查局项目"武夷山松溪—庆元地区区域地质调查"(DD20190045)资助。

作者简介：朱清波，男，1986年生，助理研究员，构造地质学专业，长期从事造山带地质调查研究工作；E−mail: zhuqingbo1234@163.com。

attribute and geodynamic process of the late Mesozoic in central South China. Based on a systematic analysis of the geochronology from La−MC−ICP−MS zircon U−Pb, Lu −hf isotopes and element geochemistry of the Lingshang ultramafic rocks, the authors investigated the intrusion, the source area characteristics of the ultramafic intrusion and the tectonic background reflected by them. Lingshang ultramafic intrusion suffered no significant crustal contamination. The content of MgO is concentrated with no obvious linear relationship with TiO_2, Al_2O_3, Ni, Th, and some other components, implying no significant crystallization differentiation. However, the range of Mg# and La−Sm differentiation indicates that heap crystallization and partial melting might have exerted an effect on magmatic evolution. The characteristics of rare earth and trace elements (Nb, Ta, Zr, Hf, etc.) are similar to those of intraplate basalt (OIB), and the characteristics of low SiO_2, high Ti, high Fe/Mn ratio and Ni are all closely related to asthenosphere mantle. However, the $\varepsilon_{Hf}(t)$ of zircons (6.83−11.41) are less than the value of the depleted mantle, and Nb/Ta ratios are close to the ratio of lithospheric mantle, suggesting low degree partial melting of spinel peridotite mantle source region in the relevant element diagram. All of these data suggest that the Lingshang ultramafic intrusion may be the result of the interaction between asthenosphere mantle and lithospheric mantle under the background of late Mesozoic intracontinental extension. The upwelling asthenosphere material led to the low−degree partial melting of the preexisting spinel peridotite mantle source area, and the deep ultramafic magma was emplaced rapidly along the tectonic weak zone to form the Lingshang ultramafic intrusion.

Key words: ultramafic rocks; Late Mesozoic; lithospheric extensional thinning; OIB; geological survey engineering; Jiangxi Province

About the first author: ZHU Qingbo, male, born in 1986, assistant researcher, majors in survey and study of Orogenic belt; E−mail: zhuqingbo1234@163.com.

Fund support: Supported by the project of China Geological Survey(No. DD20190045).

1 引　言

华南板块由扬子和华夏两大块体在新元古代—早古生代逐渐碰撞拼贴而成为统一的块体,二者以钦杭结合带相分隔,大致沿绍兴—江山—广丰—萍乡向西南延伸至钦州湾一带。钦杭带不仅是一条巨型的构造−岩浆活动带,也是华南地区最为重要的多金属成矿带,分布着一大批特大型Cu−Au−Ag−Pb−Zn−Nb−Ta−U矿床(毛景文等, 2011; 倪培等, 2017)。近年来,前人从构造变形、盆地性质、地幔属性、地球物理和深部构造等方面对钦杭结合带乃至华南晚中生代构造−岩浆事件的动力学背景进行了广泛研究(杨明桂等, 2009; Wang et al., 2012; Li et al., 2013; 严加永等, 2019)。

华南内部广泛分布的晚中生代A型花岗岩和碱性侵入岩(王德滋等, 1995)、板内基性岩脉(Li, 2000)、双峰式火山岩(章邦桐等, 2002)、拉分盆地(Li, 2000; 舒良树等, 2002)和变质核杂岩(Lin et al., 2000)等表明,华南内部在晚中生代发生了大规模的岩石圈伸展减薄事件(Li, 2000; 范蔚茗等, 2003)。但关于晚中生代伸展作用的构造背景尚存在两种主要的不同观点:古太平洋板块俯冲−后撤所导致的弧后伸展模式(Li, 2000; Wang et al., 2006a; Li et al., 2007)和板内岩石圈伸展模式(毛景文等, 1998; 王岳军等, 2004)。

可见理解华南内部中生代岩浆活动是弧岩浆作用还是陆内岩石圈伸展减薄作用的产物,对认识华南中生代构造演化具有重要的作用。晚中生代华南以大规模分布的火山−侵入杂岩为特征,其主要岩浆作用时间集中在180~160 Ma、160~135 Ma和135~90 Ma三个阶段。目前对华南内部中生代岩浆活动的研究多集中在火山岩、中基性侵入岩和花岗岩等(Li et al., 2007),对于超镁铁质岩的报道则较为稀少。超镁铁质岩起源于地球深部的地幔,是深源岩浆侵位的产物,形成于不同构造环境(如大洋盆地或弧后盆地、俯冲带及陆内环境等)的镁铁质—超镁铁岩具有不同的岩石地球化学特征,是研究地幔属性及地球深部动力学过程的良好对象。最近,笔者对出露于钦杭结合带东段赣北新余地区的岭上超镁铁岩体进行了锆石La−MC−ICP−MS U−Pb、Lu−Hf同位素测试和岩石地球化学研究,厘定出早白垩世(120 Ma)具有OIB特征的超镁铁质堆晶岩,认为其形成于早白垩世晚期的板内伸展环境,对于认识华南中部晚中生代地幔源区特征及大地构造

背景具有重要意义。

2　地质概况

钦杭结合带是扬子地块与华夏地块在晋宁期—加里东期多岛弧碰撞、拼贴形成的结合带，西起广西钦州湾，北至浙江杭州湾，总体呈反S形弧状展布(杨明桂等, 1997)，北以宜丰—景德镇—歙县断裂为界，南以萍乡—广丰—江山—绍兴断裂与华夏地块分隔，其中钦杭结合带东段主体为一套新元古代活动大陆边缘火山—沉积建造。早古生代之后进入被动大陆边缘演化阶段，经历了多期构造活动的叠加改造(徐先兵等, 2015; 宋传忠等,2019)。海西期发生陆内裂陷形成萍乡—钱塘坳陷带，印支—燕山期发生强烈的陆内造山活动。晚中生代构造体制反转，由陆内造山转换为岩石圈伸展减薄的构造环境，导致大规模的A型和双峰式岩浆活动、基性—超基性岩侵位、伸展断陷盆地(K_2—E)、变质核杂岩及岩浆成矿作用的大爆发(图1)。

对应于多期不同性质的构造-岩浆活动，在钦杭结合带发育有多期基性—超基性岩：(1)新元古代与俯冲洋壳、岛弧和弧后盆地相关的基性—超基性岩，如：赣东北蛇绿混杂岩带中的基性—超基性岩块(Zhang et al.,2015)；(2)加里东期与俯冲相关的火山弧或活动大陆边缘的基性—超基性岩，如：松溪辉长岩(Zhang et al.,2016)；(3)中生代形成于板内伸展背景的基性—超基性岩，基本上都沿区域性断裂带发育，如：龙游和衢州的超基性岩(Qi et al., 2016)；(4)中新生代超基性岩体岩筒和基性岩脉。

其中新余地区超镁铁质岩体出露于钦杭结合带东段广丰—萍乡断裂带内，一系列岩体呈近东西

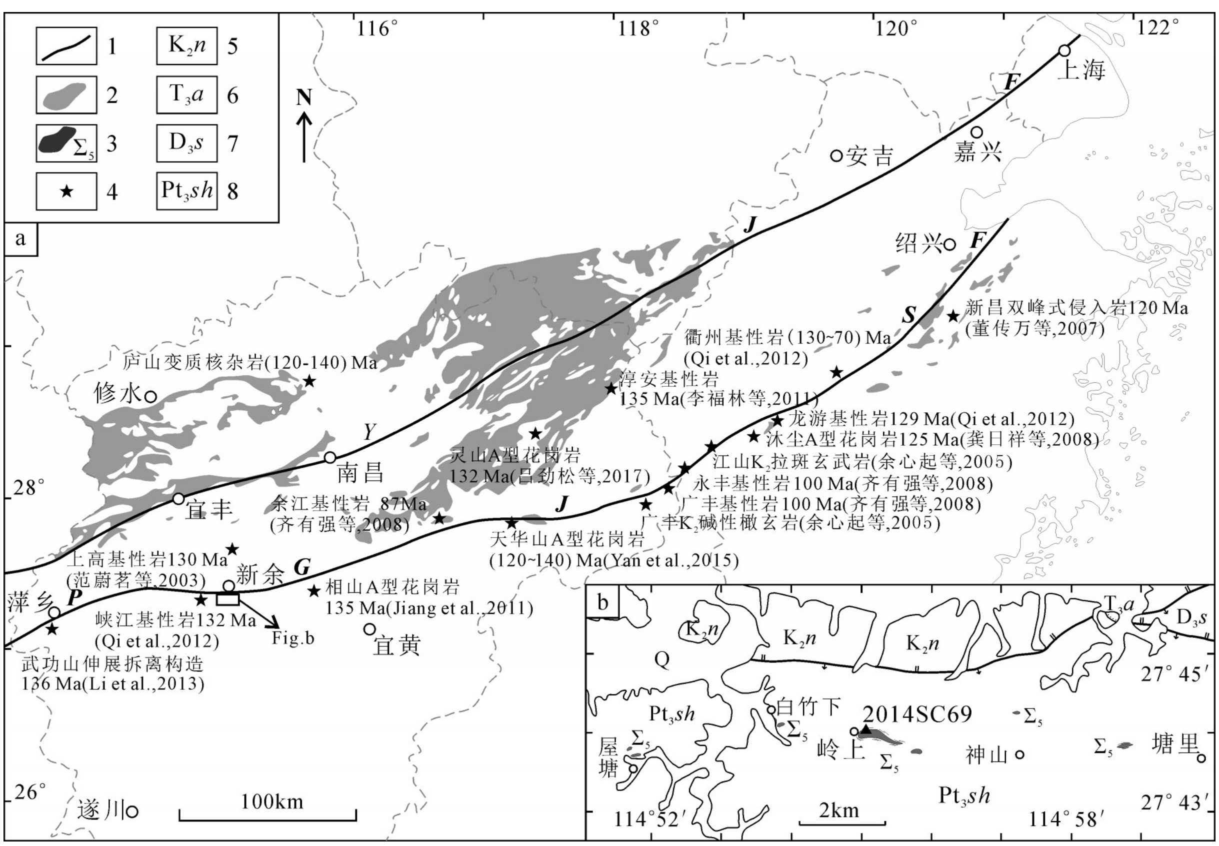

图1 钦杭结合带东段地质简图(a)和岭上超镁铁岩体地质简图(b)

1—钦杭结合带；2—前寒武基底；3—超镁铁岩；4—晚中生代基性岩/A型花岗岩/伸展构造；5—南雄组；6—安源组；7—佘田桥组；8—神山组

YJF—宜丰—景德镇断裂；PGJSF—萍乡—广丰—江山—绍兴断裂

Fig. 1 Geological schematic map of Qinzhou–Hangzhou juncture belt (a) and Lingshang ultramafic intrusion (b)

1–Qinzhou–Hangzhou junction belt; 2–Precambrian basement; 3–Ultramafic; 4–Late Mesozoic basic rock/A–type granite/extensional structure; 5–Nanxiong Formation; 6–Anyuan Formation; 7–Shetianqiao Formation; 8–Shenshan Formation

YJF–Yifeng–Jingdezhen Fault; PGJSF–Pingxiang–Guangfeng–Jiangshan–Shaoxing Fault

向串珠状展布于塘里—神山—岭上—白竹下—屋塘等地,断续出露长15 km,单个岩体形态也呈近东西向。其中岭上超镁铁岩体出露面积最大(约0.15 km²),呈岩墙状侵入新元古代神山群浅变质的碎屑岩中,向北倾斜且东西向尖灭,可见冷凝边和围岩的热接触变质现象(赖新平, 1989)。岭上岩体主要由蛇纹石化(辉石)角闪橄榄岩和蛇纹石–滑石化辉石橄榄岩组成,岩体边部为辉石角闪岩、绿泥石化角闪石岩和透闪石化辉长辉绿岩。其中本文所取样品为该岩体的超镁铁单元,岩石呈灰绿至暗绿色,致密块状构造,发生了强烈的蛇纹石化、透闪石化、滑石化和碳酸盐化,橄榄石和辉石假晶仍保留其较自形的粒状和短柱状,并含有少量的磷灰石和磁铁矿(图2)。

3 分析方法及结果

3.1 分析方法

用于锆石U–Pb定年、Lu–Hf同位素分析的样品均采自岩体内部无明显变质蚀变和脉体穿插的部位。锆石的分选工作在河北省廊坊宇能岩石矿物分选技术服务有限公司完成,样靶制备和锆石阴极发光照相在北京锆年领航制靶公司完成。

锆石LA–MC–ICP–MS U–Pb定年在天津地质矿产研究所同位素实验室进行,等离子质谱仪为Thermo Fisher公司制造的Neptune,激光器为美国ESI公司生产的UP193–FX ArF准分子激光器。在分析过程中,激光剥蚀的斑束直径选为32 μm,频率为8~10 Hz,以He作为剥蚀物质的载气。应用NIST612玻璃作为元素外标,锆石标样GJ–1进行同位素分馏校正,锆石标样Mud Tank作为同位素监控样。具体分析方法及仪器参数见文献(彭戈等, 2012)。

锆石Lu/Hf同位素分析在天津地质矿产研究所同位素实验室的多接收器电感耦合等离子体质谱仪(NEP TUNE)和氟化氩准分子激光器(NEW WAVE 193 nm EX)上进行,详细的实验分析过程见文献(耿建珍等, 2011)。对已完成U–Pb同位素分析

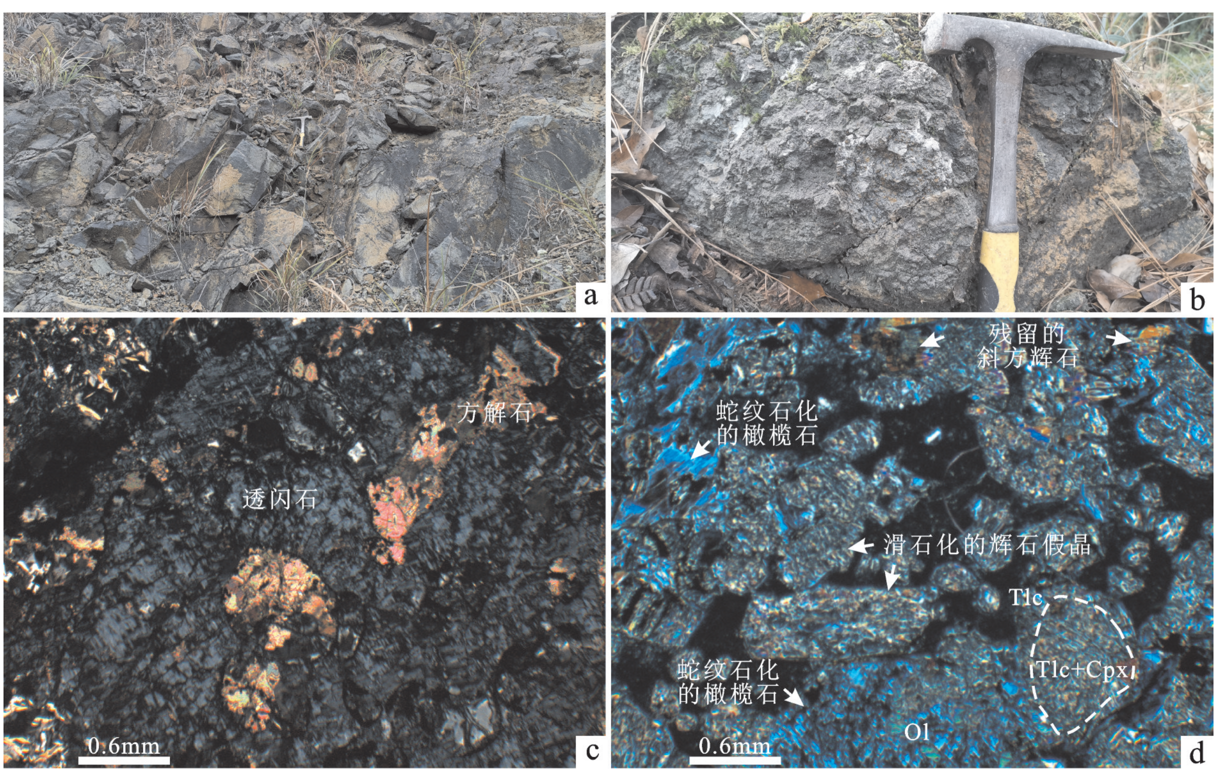

图2 岭上超镁铁岩野外和显微照片

a—岭上超镁铁岩露头特征;b—岭上超镁铁岩手标本特征;c,d—岭上超镁铁岩显微特征

Fig. 2 Field photographs and Microscopic photographs of ultramafic rocks from Lingshang ultramafic intrusion

a–Outcrop characteristic of Lingshang ultramafic rock; b–Hand specimens characteristics of Lingshang ultramafic rock; c, d–Microscopic characteristics of Lingshang ultramafic rocks

的锆石进行Lu/Hf同位素分析，激光剥蚀的斑束直径为50 μm或75 μm，能量密度为10~11 J/cm^2，频率为8~10 Hz。在实验过程中，标准锆石GJ-1和MUD的^{176}Hf/^{177}Hf加权平均值均与已报道值相一致(Morel et al., 2008)。

全岩主量元素和微量元素组成分析在中国科学院贵阳地球化学研究所完成。主量元素分析使用仪器为Rigaku ZSX100e XRF。微量元素和稀土元素测定仪器为Bruker M90 ICP-MS，仪器灵敏度调整到1 ng/mL^{115}In约30000 cps。方法以多元素标准溶液(AccuStandard Inc，USA)作为外标，以国际标样AMH-1(安山岩)和OU-6(板岩)作为标准参考物质。大部分元素的相对误差优于(±5)%，具体步骤见(Qi et al., 2000)。

3.2 分析结果

3.2.1 锆石LA-ICP-MS U-Pb年龄

本次工作对蛇纹石化橄榄辉石岩中的32颗锆石进行了锆石U-Pb分析，其中绝大多数锆石的^{206}Pb/^{238}U年龄位于114~130 Ma(图3a)，锆石粒径在100~150 μm，绝大多数呈较自形的短柱状，长宽比<2。阴极发光图像(图3b)显示锆石内部多具有与晶体边界一致的、宽的震荡环带或无环带构造，部分锆石内部具有扇形分带结构，其外部同样发育较宽的结晶环带；^{232}Th/^{238}U比值为0.46~1.60，>0.1且变化范围较大与典型的超镁铁岩中的锆石一致(表1)。其^{206}Pb/^{238}U加权平均年龄为(120.8±1.4)Ma(n=28, MSWD =4.2)，代表了该超基性岩的结晶年龄。此外，该超镁铁质岩中还含有少量的捕获锆石，其^{206}Pb/^{238}U年龄分别为(1976±29)Ma、436~442 Ma和(181±2)Ma(图3a、b)。

3.2.2 锆石Lu-Hf同位素

对岭上超镁铁岩中的13颗锆石进行了Lu-Hf同位素分析，其中岩浆结晶锆石(^{206}Pb/^{238}U年龄在114~127 Ma)的^{176}Hf/^{177}Hf比值变化范围较小，集中在0.282909~0.283031 (平均值为0.282958)，其对应的$\varepsilon_{\rm Hf}(t)$在6.83~11.41 (平均值为8.71)(图3c)，$T_{\rm DM1}$年

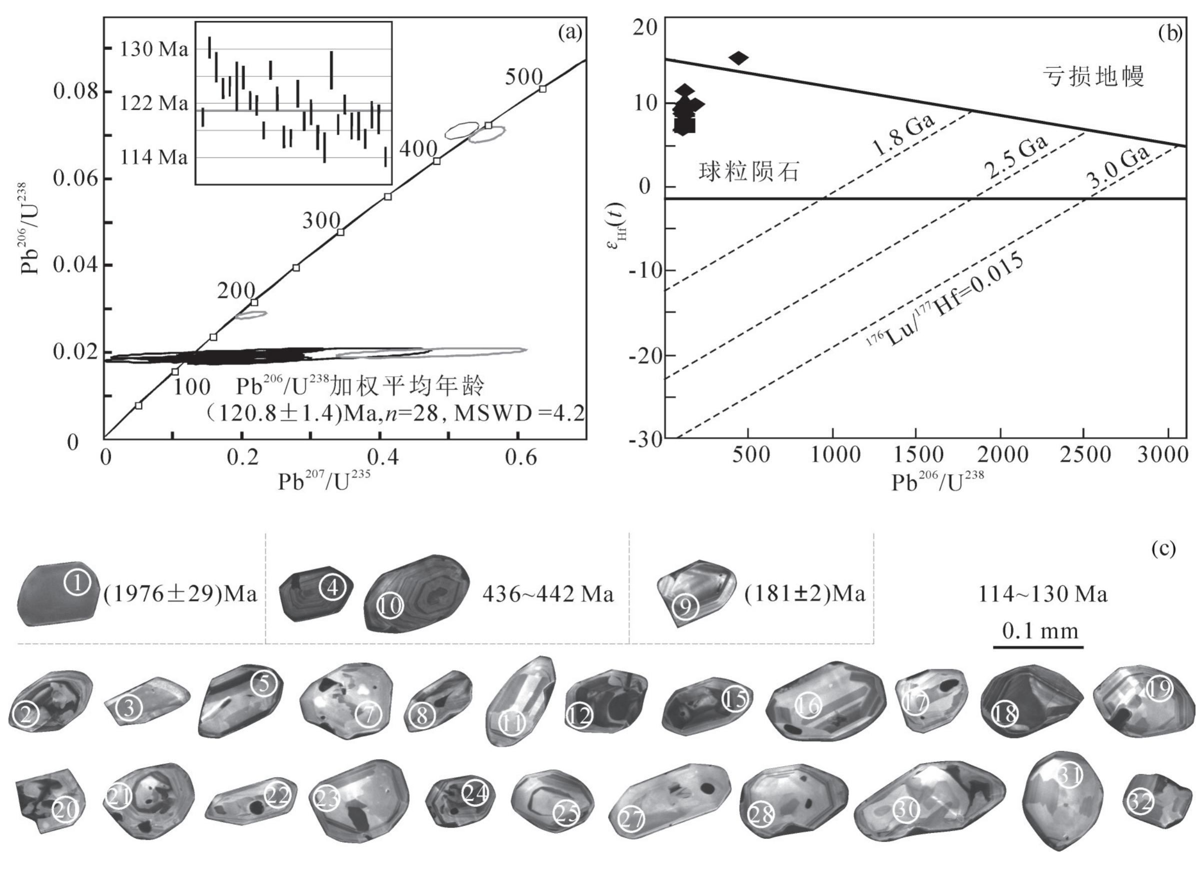

图3 锆石U-Pb年龄谐和图(a)、锆石$\varepsilon_{\rm Hf}(t)$图解(b)、锆石阴极发光特征(c)

Fig.3 The zircon U-Pb concordia diagrams (a), probabilistic histogram of age distributions of zircons and $\varepsilon_{\rm Hf}(t)$ versus (b), the character of CL images for zircon (c)

表1 岭上超镁铁岩锆石U−Th−Pb同位素分析结果

Table 1 Analytical results of U−Th−Pb isotopes for intrusion of Lingshang

样品号	含量/10^{-6}		同位素比值					年龄/Ma					
2014SC69	Th	U	$^{206}Pb/^{238}U$	$^{207}Pb/^{235}U$	$^{207}Pb/^{206}Pb$	$^{208}Pb/^{232}Th$	$^{232}Th/^{238}U$	$^{206}Pb/^{238}U$	1σ	$^{207}Pb/^{235}U$	1σ	$^{207}Pb/^{206}Pb$	1σ
1	26	7	0.3588	42.1706	0.8524	0.2317	3.6275	1976	29	3823	79	5012	30
2	501	529	0.0188	0.1772	0.0684	0.0083	0.9469	120	1	166	7	881	91
3	473	316	0.0204	0.2765	0.0983	0.0090	1.4999	130	2	248	16	1591	119
4	691	672	0.0700	0.5556	0.0575	0.0241	1.0284	436	5	449	9	513	38
5	94	203	0.0200	0.2271	0.0825	0.0122	0.4640	127	2	208	26	1258	252
6	344	414	0.0195	0.1281	0.0477	0.0070	0.8315	124	2	122	7	86	143
7	309	275	0.0195	0.1539	0.0572	0.0080	1.1233	125	1	145	18	499	277
8	79	90	0.0195	0.3188	0.1185	0.0092	0.8807	125	4	281	56	1934	596
9	345	369	0.0285	0.2134	0.0543	0.0089	0.9353	181	2	196	8	383	94
10	409	456	0.0709	0.5195	0.0531	0.0219	0.8966	442	5	425	8	333	42
11	132	159	0.0197	0.1556	0.0572	0.0061	0.8307	126	2	147	17	501	250
12	1224	999	0.0192	0.1387	0.0524	0.0060	1.2251	122	1	132	4	305	63
13	1169	915	0.0191	0.1715	0.0652	0.0065	1.2781	122	1	161	5	782	62
14	1120	699	0.0185	0.1494	0.0586	0.0055	1.6010	118	1	141	5	553	77
15	574	479	0.0199	0.2626	0.0958	0.0075	1.1974	127	1	237	9	1544	74
16	129	136	0.0192	0.1742	0.0657	0.0056	0.9515	123	2	163	22	798	289
17	161	153	0.0183	0.1314	0.0520	0.0057	1.0488	117	2	125	18	285	338
18	664	539	0.0183	0.1729	0.0685	0.0058	1.2303	117	1	162	10	885	122
19	92	131	0.0193	0.1325	0.0497	0.0068	0.7028	123	2	126	47	182	978
20	436	370	0.0187	0.1296	0.0503	0.0052	1.1756	119	1	124	8	208	147
21	103	150	0.0189	0.2349	0.0901	0.0089	0.6844	121	2	214	21	1428	189
22	141	159	0.0183	0.2295	0.0909	0.0051	0.8832	117	2	210	22	1444	207
23	78	89	0.0181	0.2121	0.0851	0.0054	0.8732	116	2	195	33	1317	355
24	66	99	0.0199	0.4755	0.1735	0.0102	0.6703	127	3	395	47	2591	208
25	233	234	0.0186	0.1377	0.0536	0.0049	0.9950	119	1	131	15	355	258
26	338	351	0.0191	0.2045	0.0777	0.0059	0.9630	122	1	189	11	1139	120
27	163	172	0.0186	0.1232	0.0481	0.0051	0.9471	119	2	118	23	104	576
28	88	103	0.0186	0.1455	0.0568	0.0058	0.8527	119	2	138	56	484	1013
29	324	379	0.0183	0.1869	0.0741	0.0046	0.8541	117	1	174	8	1045	101
30	195	209	0.0188	0.1506	0.0579	0.0058	0.9320	120	2	142	33	528	549
31	83	94	0.0187	0.1635	0.0633	0.0043	0.8837	120	2	154	27	718	437
32	330	263	0.0179	0.1551	0.0630	0.0040	1.2564	114	1	146	13	708	184

龄在0.31~0.50 Ga。两颗捕获锆石的$\varepsilon_{Hf}(t)$为较高的正值，分别为15.35($^{206}Pb/^{238}U$年龄约442 Ma)和9.74($^{206}Pb/^{238}U$年龄约181 Ma)，其对应的T_{DM1}年龄均为0.43 Ga，与结晶锆石的一阶段模式年龄相一致(表2)，反映源区可能存在加里东期的岩石圈地幔。表明该超镁铁岩的源区可能存在加里东期新生的岩石圈地幔。

3.2.3 风化蚀变影响

已有研究表明碱金属元素(Ca、Na、K)和大离子亲石元素(Rb、Sr、Ba等)具有极高的活动性(Wang et al., 2006b)，在热液蚀变过程中会发生不同程度的改变。而一些活动性较差的主量元素(Si、Al、P、Mn、Fe)、过渡元素(Sc、V、Cr、Co、Ni、Y、Zr、Nb、Mo、La、W)、HREE和高场强元素(HFSE：Nb、Ta、Zr、Hf、U、Th、Ce、Ti等)活动性很低(Smith et al., 1976)，在大多数的风化和热液蚀变过程中不易迁移(Hawkesworth et al., 1997)，元素含量和比值基本不发生改变。

火成岩的烧失量(LOI)可以反映其遭受风化和蚀变的程度(Wang et al., 2006b; Wang et al., 2015)。岭上超镁铁岩有较明显的蛇纹石化、透闪石化和不同程度的碳酸盐化等蚀变,与样品具较高的烧失量一致。其中Na_2O、K_2O和LOI之间具有一定的相关性,在稀土元素配分曲线中Rb、Ba、Sr呈现明显的负异常,表明岩石遭受了一定的后期蚀变,上述元素可能存在较明显的流失。虽然富含橄榄石和辉石的镁铁质—超镁铁质岩在蚀变过程中Mg较易发生迁移,但岭上超镁铁岩各样品的MgO含量非常集中,且MgO、Nb、La和Zr与LOI之间没有明显的相关性,可以排除低温蚀变对MgO、稀土元素和高场强元素的影响,没有明显的Ce异常也表明不相容元素和同位素比值没有受到蚀变的显著影响(Deniel, 1998)。因此文中仅使用上述在蚀变过程中未发生明显迁移的部分主量元素、高场强元素、稀土和过渡元素等进行讨论。

3.2.4 地球化学特征

岭上岩体超镁铁岩由辉石、橄榄石及少量的斜长石和铬铁矿组成,发生了强烈的蛇纹石化和绿泥石化。各主量元素含量比较一致,具低SiO_2(39.32%~43.62%,平均为41.16%,仅1个样品2014SC69H9的SiO_2含量很低可能是受局部强堆晶作用的影响)、高MgO(23.7%~31.49%)和Fe_2O_3T(12.66%~15.08%,平均值为13.08%)含量的特征。Al_2O_3和CaO的含量较低,分别为5.38%~7.28%(原始地幔值为3.97%),2.27%~3.8%(原始地幔值为3.5%)。$Mg^{\#}>68$ (Green, 1975; Freg et al., 1978; Hess, 1992)是鉴别原生岩浆的重要标志之一,岭上岩体的$Mg^{\#}$值在79~85(表3),主要由岩浆早期结晶的矿物相聚集而成。在Miyashiro(1974)针对火山岩所做的$SiO_2-Fe_2O_3T/MgO$图解中(图4b),岭上超镁铁岩位于拉斑玄武岩系列区。在$Al_2O_3-CaO-MgO$图解上均位于超镁铁质堆晶岩的区域(图4a),与其岩相学特征相一致。其烧失量较大(8.18%~11.37%),大离子亲石元素(K、Na、Rb、Ba等)可能存在较明显的迁移流失。

岭上超镁铁岩的稀土元素总量∑REE在23.8×10^{-6}~29×10^{-6}。经球粒陨石标准化的稀土配分曲线(图5a)向右缓倾,轻稀土富集$(La/Yb)_N$=5.2~8.7,$(La/Sm)_N$=2.44~4.94,$(Gd/Yb)_N$=1.52~2.06,轻重稀土分异明显,重稀土之间分异程度较低,Tb−Lu段的标准化曲线非常平缓。具极弱的Eu正异常(Eu*在1~1.18),类似于洋岛玄武岩(OIB),未遭受明显的地壳混染。

岭上超镁铁岩微量元素的原始地幔标准化曲线中(图5b),各样品的微量元素组成曲线基本平行,暗示岩浆源区的统一性。Cr(1413×10^{-6}~2167×10^{-6})、Ni(927×10^{-6}~1170×10^{-6})较高指示了岩浆具幔源属性。无显著的Zr、Hf和Ti异常,Nb和Ta富集,除Rb、Ba和Sr外,曲线形态与OIB非常类似。大部分样品具有负Sr异常和Rb、Ba变化较大的特点,可能与岩石较强的蚀变有关。2件样品出现微弱的Sr正异常,可能与其局部斜长石的含量有关(图5b)。MgO的含量比较集中,TiO_2、CaO、Al_2O_3、Ni、Cr、Sr、

表2 锆石Lu−Hf同位素组成

Table 2 Analytical results of Lu−Hf isotopes for zircons

点号	年龄/Ma	$^{176}Hf/^{177}Hf$	±1σ	$^{176}Lu/^{177}Hf$	$^{176}Yb/^{177}Hf$	$(^{176}Hf/^{177}Hf)_i$	$\varepsilon_{Hf}(t)$	±1σ	T_{DM1}/Ga
5	127	0.282911	0.000012	0.0008	0.0312	0.282909	7.21	0.42	0.48
6	124	0.282954	0.000013	0.0012	0.0414	0.282951	8.63	0.46	0.42
9	181	0.282953	0.000019	0.0019	0.0541	0.282947	9.74	0.67	0.43
10	442	0.282948	0.000012	0.0009	0.0293	0.282941	15.35	0.42	0.43
11	126	0.283031	0.000014	0.0011	0.0429	0.283028	11.41	0.49	0.31
12	122	0.282956	0.000013	0.0012	0.0445	0.282953	8.66	0.44	0.42
13	122	0.282992	0.000018	0.0022	0.0789	0.282987	9.85	0.61	0.38
14	118	0.282909	0.000019	0.0023	0.0929	0.282904	6.83	0.47	0.50
23	116	0.282974	0.000012	0.0005	0.0186	0.282973	9.22	0.42	0.39
24	127	0.282913	0.000010	0.0005	0.0175	0.282912	7.30	0.33	0.47
28	119	0.282970	0.000010	0.0005	0.0180	0.282969	9.15	0.35	0.39
30	120	0.283000	0.000014	0.0007	0.0266	0.282998	10.21	0.49	0.35
32	114	0.282924	0.000016	0.0011	0.0355	0.282922	7.36	0.56	0.47

表3 岭上超镁铁岩体的主量(%)和微量(10^{-6})元素

Table 3 Major (%) and trace element (10^{-6}) compositions of Lingshang ultramafic intrusion

	H1	H2	H3	H4	H5	H6	H7	H8	H9	H10
SiO_2	40.36	43.62	39.32	40.27	41.82	41.89	41.47	41.18	32.62	42.17
Na_2O	0.12	0.13	0.12	0.10	0.13	0.10	0.11	0.04	0.02	0.10
MgO	26.40	25.46	26.90	25.90	25.57	25.71	26.42	25.23	31.49	23.70
Al_2O_3	5.92	5.67	5.97	5.86	6.29	5.51	6.45	5.82	7.28	6.27
P_2O_5	0.14	0.12	0.12	0.12	0.11	0.12	0.11	0.11	0.11	0.14
K_2O	0.11	0.11	0.10	0.12	0.07	0.07	0.09	0.05	0.01	0.10
CaO	2.94	2.80	2.78	2.83	2.98	2.58	2.93	2.61	2.75	2.27
TiO_2	0.55	0.49	0.57	0.55	0.60	0.54	0.51	0.47	0.51	0.51
MnO	0.19	0.17	0.20	0.18	0.18	0.18	0.18	0.17	0.18	0.18
Fe_2O_3T	14.43	13.23	15.08	14.55	13.85	14.34	12.85	13.34	13.50	14.00
LOI	8.99	8.46	8.49	9.21	8.18	9.08	8.79	11.10	11.37	10.43
Total	100.14	100.27	99.64	99.67	99.79	100.11	99.91	100.11	99.84	99.87
$Mg^{\#}$	81.0	81.8	80.6	80.6	81.1	80.7	82.7	81.5	84.5	79.8
Li	13.7	17.8	17	14.9	17	18.5	14.5	7.15	6.73	21.4
Be	0.36	0.43	0.36	0.33	0.46	0.3	0.35	0.17	0.15	0.33
Sc	15.2	13.8	15.3	14.2	20.9	15.5	14.8	14.1	14.3	15.4
V	113	103	107	112	135	115	101	97.6	112	118
Cr	1553.1	1413.6	1478.7	1655.4	2166.9	1897.2	1553.1	1376.4	1776.3	1636.8
Co	98.2	91.9	101	106	107	104	103	90.8	94.3	93.6
Ni	1000	927	1060	1140	1100	1170	1040	954	935	1150
Cu	57.9	39.8	15	71.7	12.9	28.9	37.5	34.3	23.3	31.1
Zn	109	101	116	144	107	115	114	111	110	127
Ga	6.86	6.24	6.31	7.27	6.92	6.92	6.6	7.12	6.52	8.23
Rb	5.68	5.04	2.55	5.69	3.13	2.39	4.28	0.9	0.63	3
Sr	83.7	39.1	34.4	76.5	48.9	31.7	44.4	200	185	34.1
Y	6.4	6.45	6.24	7.24	6.87	6.21	6.25	6.07	6.64	6.39
Zr	38.8	40.6	35.9	38.5	36.9	39.2	34.7	38.8	41.1	31.6
Nb	7.34	6.91	6.79	8.22	8.36	7.3	6.93	6.59	6.54	6.88
Cs	12	17.2	13.7	8.9	7.1	6.04	10.1	0.28	0.26	1.89
Ba	22.5	29.1	26.8	21.4	20.9	12.8	19	8.97	7.64	24.9
La	5.23	4.24	5.78	6.08	5.3	4.94	4.85	5.06	5.29	5.89
Ce	9.6	8.38	10.1	10.6	10.5	8.86	9.33	9.76	10.5	10
Pr	1.11	1.09	1.23	1.33	1.32	1.15	1.19	1.17	1.27	1.36
Nd	4.58	4.54	4.82	5.28	5.65	5.06	5.2	4.91	5.42	5.83
Sm	1.09	1.12	0.95	1.28	1.29	1.07	1.16	1.06	1.16	1.3
Eu	0.39	0.41	0.38	0.44	0.43	0.37	0.39	0.41	0.43	0.47
Gd	1.169	1.088	1.082	1.247	1.285	1.158	1.146	1.047	1.078	1.237
Tb	0.21	0.19	0.2	0.2	0.22	0.19	0.2	0.18	0.2	0.2
Dy	1.21	1.15	1.17	0.96	1.24	1.11	1.13	1.03	1.12	1.12
Ho	0.24	0.25	0.25	0.24	0.27	0.26	0.24	0.24	0.27	0.27
Er	0.64	0.59	0.6	0.58	0.72	0.63	0.63	0.61	0.65	0.66
Tm	0.095	0.09	0.1	0.09	0.1	0.09	0.09	0.08	0.1	0.09
Yb	0.56	0.58	0.59	0.5	0.64	0.57	0.56	0.5	0.57	0.53
Lu	0.09	0.09	0.09	0.1	0.1	0.1	0.09	0.09	0.09	0.08
Hf	0.91	0.96	0.92	1.18	0.92	0.87	0.83	0.82	0.84	0.74
Ta	0.6	0.45	0.54	1.18	0.63	0.59	0.65	0.54	0.51	0.54
W	1.6	1.17	1.6	6.51	0.55	0.99	1.38	2.09	1.09	1.26
Tl	0.04	0.06	0.05	0.09	0.02	0.02	0.02	0.01	0.01	0.02
Pb	1.46	1.06	1.43	1.49	2.09	1.71	1.58	1.64	1.53	1.09
Bi	0.021	0.024	0.018	0.018	0.032	0.026	0.035	0.032	0.029	0.017
Th	1.03	0.75	0.84	0.76	1.19	1.27	1.07	0.99	1.15	0.77
U	0.22	0.15	0.18	0.19	0.18	0.21	0.19	0.22	0.23	0.14

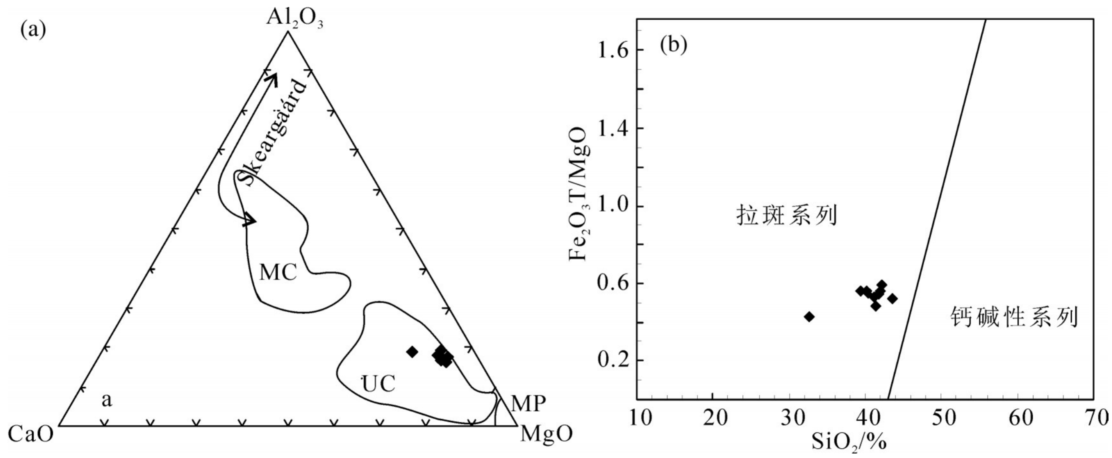

图4 岭上岩体超镁铁岩 Al_2O_3−MgO−CaO图解(a, 据Coleman, 1977)和 SiO_2−Fe_2O_3T/MgO图解（b）
MP—地幔岩; UC—超镁铁堆晶岩; MC—镁铁堆晶岩
Fig. 4 Diagram of Al_2O_3−MgO−CaO from Lingshang ultramafic intrusion (a, after Coleman, 1977) and SiO_2−Fe_2O_3T/MgO
Mp−Rocks from mantle; UC−Ultramafic cumulate; MC−Mafic cumulate

Th和MgO之间不存在明显的线性关系。

4 讨 论

4.1 形成时代

关于岭上超镁铁岩体的时代一直存在不同的认识：早期新余幅1∶5万区域地质调查(赖新平, 1989)认为其是燕山早期的超基性侵入岩，而江西地质志(1984)则认为是晋宁期超浅成次火山岩。最新修编的1∶25万宜春幅区域地质调查(2013)和江西省地质志(2015)则认为该岩体属于加里东期基性—超基性侵入岩体。本次研究表明，岭上超镁铁岩中的~120 Ma的锆石具有典型的基性岩浆锆石特征。其中加里东期锆石环带明显略呈长柱状，具有典型的中酸性岩浆锆石的特征，且数量极少(仅有2颗)，和样品中的古元古代锆石同属于典型的捕获锆石，不能代表该超镁铁岩体形成于加里东期或古元古代。因此采用La−ICP−MS锆石U−Pb定年所获得的谐和年龄(120.8±1.4)Ma(n=28，MSWD=4.2)代表了岭上超镁铁岩体的结晶年龄，属于早白垩世晚期，是华南内陆晚中生代岩石圈伸展减薄的产物。

华南中生代岩石圈伸展作用主要发生在245~230 Ma、180~175 Ma、165~142 Ma、130~101 Ma、95~85 Ma六个阶段。其中晚中生代(约120 Ma)镁铁质岩常与A型花岗岩和碱性岩相伴生形成类双峰式火成岩。早白垩世(139~123 Ma)A型花岗岩或碱性侵入岩主要分布于政和大浦断裂带以西，在钦杭结合带形成了132~123 Ma的A型花岗岩带(毛建仁等, 2014)和一系列晚古生代的基性岩墙(80~100

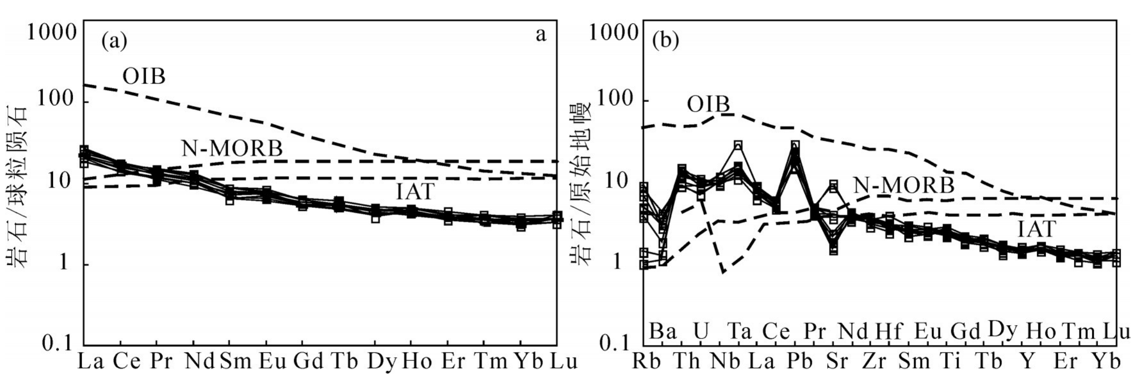

图5 岭上超镁铁岩体的稀土元素配分曲线(a)和微量元素蛛网图(b)
Fig. 5 Chondrite−normalized rare earth element (REE) patterns (a) and primitive−mantle−normalized multi−element diagrams（b）of Lingshang ultramafic intrusion

Ma)(谢桂青等，2003)。在华夏地块东南部则形成了大规模的酸性火山−侵入杂岩(145~125 Ma)和沿长乐—南澳断裂带断续分布的镁铁质侵入岩(129~100 Ma)(周金城等, 2001)。同时区域上还发育有早白垩世伸展断陷盆地和多个变质核杂岩。同期的玄武质熔岩广泛发育在早白垩世火山−沉积断陷盆地中，显示该阶段华南东部发生了显著的岩石圈伸展减薄事件。

4.2 地壳混染和结晶分异作用

评估结晶分异和地壳物质的混染是探讨岩石源区特征的重要前提。地壳混染会使岩浆的SiO_2增高和$Mg^{\#}$值显著降低，而岭上超镁铁岩SiO_2(39%~44%)含量较低，MgO含量较高，Nb−Ta富集，锆石Hf同位素强烈亏损(6.83×10^{-6}~11.41×10^{-6})，这些地球化学特征表明其形成过程中未受到明显的地壳混染。此外，一些微量元素指标常用来识别幔源岩浆是否受到地壳或岩石圈地幔物质的混染(Neal et al., 2002)。如岩石中高$(Th/Nb)_N$(>>1)和低Nb/La(<1)通常是受到地壳混染的结果(Kieffer et al., 2004)。岭上岩体的Th/Nb=0.77~1.47、Nb/La=1.12~1.57，且Th(0.75×10^{-6}~1.27×10^{-6})和U(0.15×10^{-6}~0.23×10^{-6})相比于地壳的元素含量(Th=1.2×10^{-6}~10.5×10^{-6}，U=0.2×10^{-6}~2.7×10^{-6}) (Rudnick et al., 2003)均较低。此外，在$(La/Nb)_N$−$(Th/Ta)_N$(Neal et al., 2002)图解中所有样品点接近于原始地幔和OIB区域(图6b)，而远离地壳和岩石圈地幔端元。以上特征均显示未受到明显的岩石圈地幔和地壳物质的混染。

岭上超镁铁岩的MgO含量比较集中，其与TiO_2、Al_2O_3、Ni、Cr、Sr、Th之间不存在明显的线性关系，反映该岩体未发生显著的结晶分异。但在La/La−Sm图解中(图7a)，岭上超镁铁岩具有倾斜线性分布趋势，La−Sm分异程度较高，指示部分熔融和结晶分异作用可能对岩浆的演化具有一定的影响。与地幔橄榄岩处于平衡状态的未分异初始岩浆的$Mg^{\#}$介于60~74 (Frey et al., 1978)，岭上超镁铁岩含有较高的MgO(23%~32%)和$Mg^{\#}$(79.8~84.5) > 74，反映了橄榄石和辉石一定程度的堆晶作用。岭上超镁铁岩主要由岩浆早期结晶的矿物相聚集而成，源区可能是超镁铁岩熔融的产物。稀土元素配分曲线中没有出现明显的Eu异常，表明不存在显著的斜长石结晶分异，与岩石中主要为辉石和橄榄石的矿物组成一致。

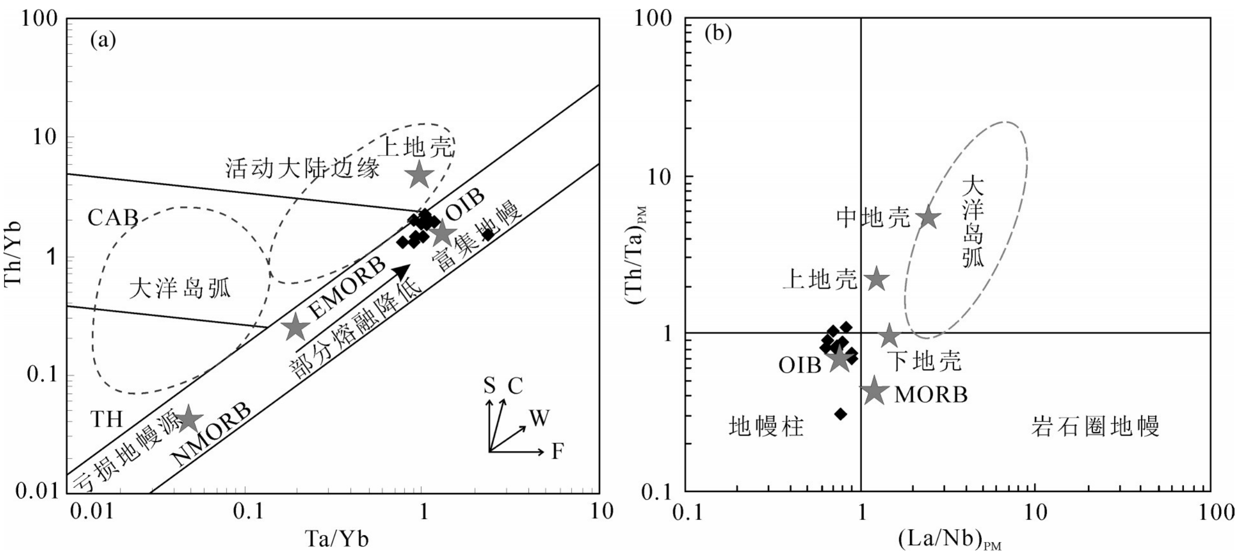

图6 岭上超镁铁岩Th/Yb−Ta/Yb图解(a) (据Pearce et al., 1995)和 $(La/Nb)_{PM}$− $(Th/Ta)_{PM}$图解(b)(据Neal et al., 2002)

TH—拉斑玄武岩; CA—钙碱性玄武岩; NMORB—正常洋中脊型玄武岩; EMORB—富集洋中脊型玄武岩; OIB—洋岛玄武岩; 矢量箭头分别表示俯冲组分(S)，板内富集(W)，结晶分异(F)和地壳混染(C)的影响

Fig. 6 Diagram of Ta/Yb versus Th/Yb (a) (after Pearce et al., 1995) and $(La/Nb)_{PM}$ versus $(Th/Ta)_{PM}$ (b) (after Neal et al., 2002).

TH−Tholeiite; CAB−Calc−alkaline basalt; NMORB−Normal mid−ocean ridge basalt; EMORB−Enrichment mid−ocean ridge basalt; OIB−Ocean island basalt; The vector arrows show the effects of subduction components (S), intraplate enrichment (W), crystal differentiation (F), and crustal mixing (C), respectively

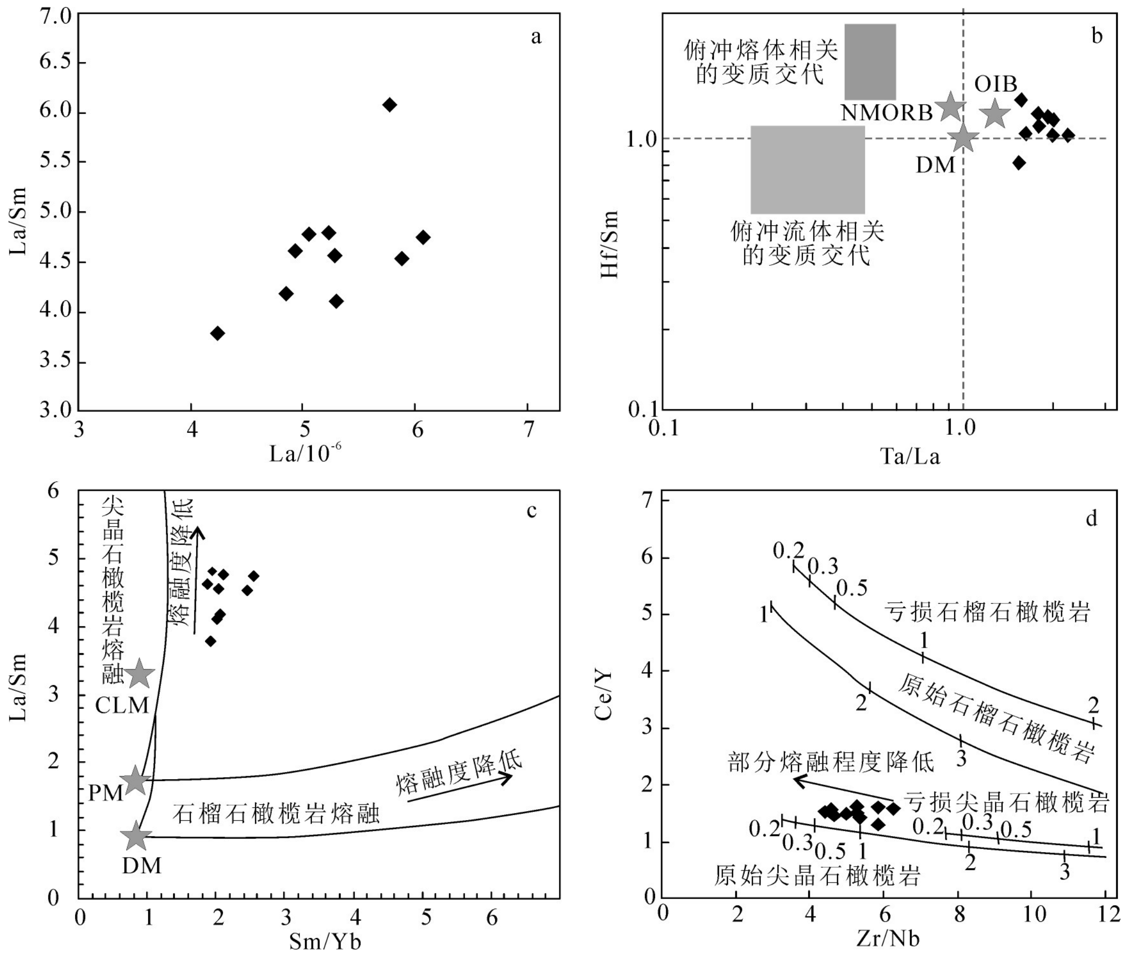

图7 La−La/Sm图解(a), Ta/La−Hf/Sm图解(b), Sm/Yb−La/Sm图解(c)和Zr/Nb−Ce/Y图解(d)(据Hardarson et al., 1991)
OIB—洋岛玄武岩;NMORB—正常洋中脊型玄武岩;CLM—大陆岩石圈地幔;PM—原始地幔;DM—亏损地幔
Fig. 7 Diagram of La−La/Sm(a), Ta/La−Hf/Sm(b), Sm/Yb−La/Sm(c) and Zr/Nb−Ce/Y(d) (after Hardarson et al., 1991)
OIB−Oceanic island basalt; NMORB−Normal mid-ocean ridge basalt; CLM−Continental lithospheric mantle; PM−Primitive mantle; DM−Depleted mantle

4.3 岩浆源区

不同构造环境下的镁铁质—超镁铁质岩浆元素地球化学特征差异明显,明确其地幔源区特征是探讨构造背景的关键。岭上超镁铁岩中岩浆结晶锆石的$\varepsilon_{Hf}(t)$在6.83~11.41 (平均值为8.71)(图3c),对应的T_{DM1}年龄在0.31~0.50 Ga,与其中捕获的早古生代锆石($^{206}Pb/^{238}U$年龄=(442±5)Ma)的Hf同位素特征较为一致($\varepsilon_{Hf}(t)$=15.35,T_{DM1}=0.43Ga),表明该超镁铁岩可能起源于先存的同位素亏损的地幔源区的部分熔融。岭上超镁铁岩中Cr (1376×10^{-6}~2167×10^{-6})、Co (90×10^{-6}~107×10^{-6})、Ni (927×10^{-6}~1170×10^{-6})略低于原始地幔的元素含量 (Rudnick et al., 2003),P_2O_5/Al_2O_3的比值为0.01~0.025,变化范围很小,反映了地幔岩部分熔融的程度很低(张贵山等, 2009)。La/Sm、Sm/Yb、Th/Yb和Ta/Yb比值受分离结晶作用影响较小,常用于判断源区性质及部分熔融的程度。在Th/Yb−Ta/Yb、La/Sm−Sm/Yb和Ce/Y−Zr/Nb图解中(图6a,图7c、d),样品均位于部分熔融程度较低的尖晶石橄榄岩区域。此外,稀土元素分馏弱及Zr−Zr/Y图解中样品相关性较差等特征也反映岭上超镁铁岩具尖晶石橄榄岩地幔源区低程度部分熔融的特征。

Nb、Ta 、Zr、Hf等具有相似地球化学特征,其比值只有在地幔源区形成的过程中才会被重置(Jochum et al.,1989;计波等,2019),是岩石成因和源区性质的示踪剂。岭上超镁铁岩的Nb/U(28.14~47.61,平均38)与OIB大致相当(37~57)(Sun et al., 1989)。在Hf/Sm−Ta/La、Ta/Yb−Th/Yb和 $(La/Nb)_{PM}$

$-$ $(Th/Ta)_{PM}$图解中也均位于OIB区域(图6,图7b)。OIB的成因通常与地幔柱活动、岩石圈伸展及大陆裂谷相关,具有OIB性质的岩浆多来源于软流圈地幔。岭上超镁铁岩具低SiO_2(绝大多数为39.32%~43.62%)和高Ti拉斑玄武岩(TiO_2=0.47%~0.6%,Ti/Y=450~550)特征,Fe/Mn比值(63.4~71.4)高于典型的上地幔值(60)(Humayun et al., 2004)而接近于地幔辉石岩和橄榄岩的Fe/Mn比值,Ni(930×10^{-6}~$1170\times10^{-6}>30\times10^{-6}$)值也与原始地幔值相一致,这些均显示出与软流圈地幔关系密切。此外,岭上超镁铁岩的Nb/La(1.17~1.63 > 1)、Hf/Ta(1~2.1 < 5)、Zr/Ba(1.2~5.4 > 0.2)和La/Ta(5.15~10.91 < 15)具有与美国盆岭地区软流圈来源的板内玄武岩(WPB)(Ormerod et al., 1988)相似的特征。但其Nb/Ta平均值为11.9,低于亏损地幔(15.5)、MORB(17.8)、OIB(17.7),接近于岩石圈地幔的Nb/Ta比值(12)(Sun et al., 1989),锆石Hf同位素的$\varepsilon_{Hf}(t)$在6.83~11.41,也未达到当时亏损地幔的程度。因此,推测岭上超镁铁岩的源区主要为亏损的软流圈地幔,并受到上覆同位素略富集的岩石圈地幔的交代。

4.4 大地构造意义

华南在中生代经历了由挤压体制向伸展体制的转换,各地构造转换的时间有所差异。南岭东段发育一系列190~175 Ma的A型花岗岩、碱性玄武岩、拉斑玄武岩和双峰式火山岩(章邦桐等, 2002),武夷山两侧发育同时期的河湖相裂陷盆地(舒良树等, 2002),在早侏罗世已处于伸展环境。而在华南内陆的赣中和赣北地区中侏罗世仍发育强烈的挤压逆冲构造(舒良树等, 2002),反映伸展构造环境的基性岩浆活动最早出现在160~170 Ma(王岳军等, 2004),在中—晚侏罗世之交(~170 Ma)才完成挤压向伸展的转换。此外,在赣湘粤地区发育T_3−J_1的前陆盆地、J_2的裂谷盆地和J_3−K的伸展断陷盆地(舒良树等,2004)。区域上,燕山早期的岩浆活动主要在扬子一侧形成挤压构造背景下成矿条件较差的S型花岗岩,而燕山晚期的岩浆活动主要在华夏一侧形成伸展环境下的与大规模成矿相关的A型花岗岩、碱性花岗岩和双峰式火山岩,也反映了华南东部中侏罗世的构造转换事件(赵希林等, 2012)。因此,华南东部应在早—中侏罗世之间完成由挤压体制向伸展体制的转换(Li et al., 2007)。晚侏罗世开始,火山−沉积盆地受到NE和EW向断裂联合控制,并以NE向伸展构造为主(余心起等, 2005)。

华南东部早白垩世(~140 Ma)以后进入全面伸展阶段,岩石圈发生强烈的伸展减薄,巨量钙碱性岩浆活动在130~100 Ma达到高潮(葛肖虹等, 2014)。在政和—大埔断裂以东沿北东向断裂形成一系列双峰式火成岩(130~100 Ma)、镁铁质岩墙群(95~85 Ma)(Li, 2000; 董传万等, 2010; 唐立梅等, 2010; 崔建军等, 2013)和碱性(A型)花岗岩(100~70 Ma) (王德滋等, 1995)。在政和—大埔断裂以西的华南内陆形成A型花岗岩类或碱性侵入岩(135~100 Ma)(王德滋等, 1995)、OIB型基性岩墙(Li, 2000)、走滑拉分−断陷盆地(Gilder et al., 1996; Li, 2000)和多个变质核杂岩(Lin et al., 2000)。其中在钦杭结合带及其周缘分布有大量同时代的长英质岩石(140~120 Ma)(Wang et al., 2013),如相山(135~137 Ma)和大茅山(122~126 Ma)等众多早白垩世A型花岗岩(Jiang et al., 2011)。但仅有少量基性—超基性岩报道(Jiang et al., 2011; Qi et al., 2016),如:钦杭结合带西段的峡江132 Ma基性岩墙、中段129 Ma辉绿岩墙侵入到A−S型花岗岩之中、东段126~129 Ma的衢州和龙游基性—超基性岩等(Jiang et al., 2011; Qi et al.,2016)及本文所报道的岭上超镁铁岩(120 Ma)。但至早白垩世晚期(112~99 Ma),软流圈来源的镁铁质岩浆在钦杭结合带的出露范围有逐渐增大的趋势(秦社彩等, 2007)。岩石圈的大规模伸展使先存的一系列北东向构造带再次活化(Zhang et al., 2013)。钦杭结合带东段的基性—超基性岩Sr−Nd同位素组成($(^{87}Sr/^{86}Sr)_i$=0.73535~0.705539,$\varepsilon_{Nd}(t)$=3~6.6)接近于亏损地幔源区(Zheng, 2012),大多不存在显著的地壳物质混染和结晶分异,可能正是与构造薄弱带岩石圈的强烈伸展加速了深部基性岩浆的侵位相关。

关于伸展的构造背景一直存在陆缘弧后伸展、造山后伸展、板内伸展等不同的观点(Li et al., 2007; Jiang et al., 2011)。已有研究表明,古太平洋板块向北西的俯冲可持续至晚白垩世(Ratschbacher et al., 2000),但华南东南部尚未发现同期的岛弧岩浆活动,即洋壳俯冲的典型产物安山质火山岩(Zheng et al., 2013)。少量玄武岩和辉绿岩墙(135~112 Ma)所表现出来的弧的特征,可能是继承了新元古代残留

洋壳(齐有强等, 2008)或岩石圈地幔的特征(Zheng et al., 2003)。钦杭结合带的侵入岩也并未呈现板片后撤模型所描述的向东南沿海变新的趋势。晚中生代基性岩遍布东南沿海和华南内陆,构造变形影响大陆板块内部上千千米,如此大范围的构造−岩浆活动难以用古太平洋板块的俯冲进行解释。华南雪峰山以东在136~97 Ma开始出现广泛的裂解,但雪峰山以西的逆冲推覆构造持续至晚白垩世,燕山晚期东张西压的构造格局也与古太平洋板块俯冲的远程效应不一致。此外,华南东部晚中生代基性岩与沿钦杭结合带分布的一系列具有板内裂谷特征的A型花岗岩一致,Sr−Nd同位素特征显示华南内部的岩石圈地幔以EMⅡ端元为主(Wang et al., 2008; 闫峻等, 2011),表现为典型的EM+OIB混合趋势(周涛发等, 2010),岭上超镁铁岩与其特征一致。可见,晚中生代华南内部处于软流圈上隆的陆内岩石圈伸展背景(范蔚茗等, 2003),多期镁铁质岩浆活动(180~85 Ma)普遍具有软流圈来源的地球化学特征,是软流圈物质上涌与富集岩石圈地幔相互作用并发生部分熔融的产物(李献华等, 1997),而非产生于俯冲带之上的构造环境(Jiang et al.,2011; Li et al.,2013)。

5 结 论

(1) 岭上超镁铁岩低SiO_2、高MgO和Nb−Ta富集、锆石Hf同位素强烈亏损等特征表明未受到明显的地壳混染。MgO含量集中且与TiO_2、Al_2O_3、Ni、Cr、Sr、Th之间不存在明显的线性关系,反映该岩体未发生显著的结晶分异。但高$Mg^{\#}$和La−Sm分异程度指示部分熔融和堆晶作用可能对岩浆的演化具有一定的影响。

(2)岭上超镁铁岩的稀土和微量元素特征类似于OIB,低SiO_2、高Ti、高Fe/Mn比值和Ni,显示与软流圈地幔关系密切。同时,其锆石$\varepsilon_{Hf}(t)$未达到亏损地幔的程度、Nb/Ta比值接近于岩石圈地幔,且在相关元素图解中具尖晶石橄榄岩地幔源区低程度部分熔融的特征。推测岭上超镁铁岩的源区主要为亏损的软流圈地幔,并受到上覆同位素略富集的岩石圈地幔的交代。

(3)位于钦杭结合带东段的岭上超镁铁岩体并非前人所认为的加里东期或新元古代岩体,其锆石U−Pb谐和年龄((120.8±1.4)Ma)代表了岭上超镁铁岩体的结晶年龄,与钦杭结合带东段早白垩世晚期一系列的伸展构造−岩浆活动相一致。其是在华南内陆晚中生代岩石圈伸展减薄的构造背景下,软流圈地幔和岩石圈地幔相互作用,深部超基性岩浆沿构造薄弱带快速侵位的产物。

References

Cui Jianjun, Zhang Yueqiao, Dong Shuwen, Jiang Boming, Xu Xianbing, Ma Licheng, Li Jianjun, Su Jinbao, Li Yong. 2013. Late Mesozoic orogenesis along the coast of Southeast China and its geological significance[J]. Geology in China, 40(1): 86−105 (in Chinese with English abstract).

Coleman R G. 1977. Ophiolite−Ancient Oceanic Lithosphere? [M]. Berlin:Springger Verlag.

Deniel C. 1998. Geochemical and isotopic (Sr, Nd, Pb) evidence for plume−lithosphere interactions in the genesis of Grande Comore magmas (Indian Ocean)[J]. Chemical Geology, 144 (3/4): 281−303.

Dong Chuanwan, Yan Qiang, Zhang Dengrong, Du Zhenyong, Zhu Guoqiang. 2010. Late Mesozoic extension in the coastal area of Zhejiang and Fujian provibces: A petrologic indicator from the Dongji island dike swarms[J]. Acta Petologica Sinica, 26(4): 1195−1203 (in Chinese with English abstract).

Fan Weiming, Wang Yuejun, Guo Feng, Peng Touping. 2003. Mesozoic mafic magmatism in Hunan−Jiangxi provinces and the lithospheric extension[J]. Earth Science Frontiers, 10(3): 159−169 (in Chinese with English abstract).

Frey F A, Green D H, Roy S D. 1978. Integrated models of basalt petrogenesis: A study of Quarti tholeiites to olivine melilities from southeastern Australia utilizing geochemical and experimental petrological data[J]. Journal of Petrology, 19(3): 463−513.

Ge Xiaohong, Liu Junlai, Ren Shoumai, Yuan Sihua. 2014. The formation and evolution of the Mesozoic−Cenozoic continental tectonics in eastern China[J]. Geology in China, 41(1):19−38 (in Chinese with English abstract).

Geng Jianzhen, Li Huaikun, Zhang Jian, Zhou Hongying, Li Huimin. 2011. Zircon Hf isotope analysis by means of LA−MC−ICP−MS[J]. Geological Bulletin of China, 30(10): 1508−1513 (in Chinese with English abstract).

Gilder Stuart, Gill James, Coe Robert, Zhao Xixi, Liu Zhongwei, Wang Genxian, Yuan Kuirong, Liu Wenlong, Kuang Guodun, Wu Haoruo. 1996. Isotopic and paleomagnetic constraints on the Mesozoic tectonic evolution of south China[J]. Journal of Geophysical Research, 101 (B7): 16137−16354.

Hardarson Björn S, Fitton J. Godfrey. 1991. Increased mantle melting beneath Snaefellsjokull volcano during Late Pleistocene glaciation[J]. Nature, 353:62−64.

Hawkesworth C J, Turner S P, McDermott F, Peate D W, Calsteren P.

1997. U−Th isotopes in arc magmas: implications for element transfer from subducted crust[J]. Science, 276: 561−555.

Humayun Munir, Qin Liping, Norman Marc D. 2004. Geochemical evidence for excess iron in the mantle beneath Hawaii[J]. Science, 306:91−94.

Ji Bo,Huang Botao,Li Xiangmin,Wang Lei. 2019.Geochronology and geochemical characteristics of the Early Ordovician granite from Hongmiaogou area in Northwest margin of South Qilian and its geological significance[J].Northwestern Geology, 52(4):63− 75(in Chinese with English abstract).

Jiangxi Bureau of Geology and Mineral Resources. 1984. Regional Geology of Jiangxi Province[M]. Beijing: Geological Publishing House(in Chinese with English abstract).

Jiangxi Bureau of Geology and Mineral Resources exploration and development. 2015. Regional Geology of Jiangxi Province[M]. Beijing: Geological Publishing House(in Chinese with English abstract).

Jiang Yaohui, Zhao, Peng, Zhou, Qing, Liao Shiyong, Jin Guodong. 2011. Petrogenesis and tectonic implications of Early Cretaceous S− and A−type granites in the northwest of the Gan−Hang rift, SE China[J]. Lithos, 121 (1−4): 55−73.

Jochum K P, McDonough W F, Palme H, Spettel B. 1989. Compositional constraints on the continental lithospheric mantle from trace elements in spinel peridotite xenoliths[J]. Nature, 340 (6234): 548−550.

Kieffer Bruno, Arndt Nicholas, Lapierre Henriette, Bastien Florence, Bosch Delphine, Pecher Arnaud, Yirgu Gezahegn, Ayalew Dereje, Weis Dominique, Jerram Dougal A., Keller Francine, Meugniot Claudine. 2004. Flood and shield basalts from Ethiopia: Magmas from the African superswell[J]. Journal of Petrology, 45(4): 793−834.

Lai Xinping. 1989. 1∶50000 Geological Map and Specification of Xinyu, Jiangxi Province[M]. Nanchang: Jiangxi Bureau of Geology and Mineral Resources Exploration and Development(in Chinese with English abstract).

Lassiter John C, DePaolo Donald J. 1997. Plume/lithosphere interaction in the generation of continental and oceanic flood basalt[C]//John J M, Millard F C (eds.). Continental, Oceanic, and Planetary Flood Volcanism. American Geophysical Union, 100: 335−355.

Li Xianhua. 2000. Cretaceous magmatism and lithospheric extension in Southeast China[J]. Journal of Asian earth Sciences, 18: 293−305.

Li Jianhua, Zhang Yueqiao, Dong Shuwen, Su Jinbao, Li Yong, Cui Jianjun,Shi Wei. 2013. The Hengshan Low− angle normal fault zone: Structural and geochronological constraints on the Late Mesozoic crustal extension in the South China[J]. Tectonophysics, 606: 97−115.

Li Zhengxiang, Li Xianhua. 2007. Formation of the 1300−km−wide intracontinental orogen and postorogenic magmatic province in Mesozoic South China: A flat−slab subduction model[J]. Geology, 35(2): 179−182.

Lin Wei. 2000. Tectonics o f SE China: New insights from the Lushan massif (Jiangxi Province)[J]. Tectonics, 19 (5): 852 −871.

Mao Jianren, Li Zilong, Ye Haimin. 2014. Mesozoic tectono−magmatic activities in South China: Retrospect and prospect[J]. Science China: Earth Sciences, 57: 2853−2877 (in Chinese with English abstract).

Mao Jingwen, Chen Maohong, Yuan Shuda, Guo Chunli. 2011. Geological characteristics of the Qinhang (or Shihang)metallogenic belt in South China and spatial−temporal distribution regularity of mineral deposits[J]. Acta Geologica Sinica, 85(5): 636−658 (in Chinese with English abstract).

Mao Jingwen, Li Hongyan, Wang Denghong. 1998. Ore−forming of Mesozoic polymetallic deposits in South China and its Relationship with Mantle Plume[J]. Bulletin of Mineralogy, Petrology and Geochemistry, 19(2): 130−132 (in Chinese with English abstract).

Meschede Martin. 1986. A method of discriminating between different type of mid−ocean ridge basalts and continental tholeiites with the Nb−Zr−Y diagram[J]. Chemical Geology, 56: 207−218.

Morel M L A, Nebel O, Nebel−Jacobsen Y J, Miller J S, Vroon P Z. 2008. Hafnium isotope characterization of the GJ−1 zircon reference material by solution and laserablation MC−ICPMS[J]. Chemical Geology, 255: 231−235.

Neal C R, Mahoney J J, Chazey W J. 2002. Mantle sources and the highly variable role of continental lithosphere in basalt petrogenesis of the Kerguelen Plateau and Broken Ridge LIP: results from ODP Leg 183[J]. Journal of Petrology, 43(7): 1177−1205.

Ni Pei, Wang Guoguang. 2017. Multiple episodes of Cu− Au mineralization in the northeastern section of the Qin− Hang metallogenic belt induced by reworking of continental crust[J]. Acta Petrologica Sinica, 33(11) : 3373− 3394 (in Chinese with English abstract).

Ormerod David S, Hawkesworth Christopher J, Rogers Nicholas W, Leeman William P, Menzies Martin A. 1988. Tectonic and magmatic transitions in the western Great Basin, USA[J]. Nature, 333(6171/6172): 349−353.

Pearce Julian A, Cann Johnson. 1973. Tectonic setting of basic volcanic rocks determined using trace element analysis[J]. Earth and Planetary Science Letters, 19: 290−300.

Pearce Julian A, Peate D W. 1995. Tectonic implications of the composition of volcanic arc magmas[J]. Annual Review of Earth and Planetary Sciences, 23:251−285.

Peng Ge, Yan Jun, Chu Xiaoqiang, Li Quanzhong, Chen Zhihong. 2012. Zircon U−Pb dating and geochemistry of Guichi intrusive rocks: Petrogenesis and deep dynamic processes[J]. Acta Petrologica Sinica, 28(10): 3271−3286 (in Chinese with English abstract).

Qi Liang, Hu Jing, Gregoire D C. 2000. Detemination of trace elements in granites by inductively coupled plasmamass spectrometry[J]. Talanta, 51:507−713.

Qi Youqiang, Hu Ruizhong, Liu Shen, M.Coulson, Qi Huawen, Tian Jianji, Zhu Jingjing. 2016. Petrogenesis and geodynamic setting of Early Cretaceous mafic−ultramafic intrusions, South China: A case study from the Gan−Hang tectonic belt[J]. Lithos, 258−259:149−162.

Qi Youqiang, Hu Ruizhong, Liu Shen, Qi Huawen, Feng Caixia. 2008. Geochemical characteristics of the mafic dikes from the Gan—Hang tectonic belt[J]. Journal of Jilin University (Earth Science Edition), 38(5): 784−794 (in Chinese with English abstract).

Qin Shecai, Fan Weiming, Guo Feng, Li Chaowen, Gao Xiaofeng. 2007. Petrogenesis of Late Mesozoic diabase dikes in Zhejiang—Fujian provinces constraints from Ar−Ar dating and geochemistry[J]. Acta Petrologica Sinica, 26(11): 3295− 3306 (in Chinese with English abstract).

Ratschbacher L, Hacker B R, Webb L E, McWilliams M, Ireland T, Dong Shuwen, Calvert A, Chateigner D, Wenk H R. 2000. Exhumation of the ultrahigh− pressure continental crust in east central China: Cretaceous and Cenozoic unroofing and the Tan—Lu fault[J]. Journal of Geophysical Research 105 (B6), 13303−13338.

Rudnick Roberta L, Gao Shan. 2003. Composition of the continental crust[J]. Treatise on geochemistry, 3: 1−64.

Rudnick Roberta L, McDonough William F, Chappell Bruce W. 1993. Carbonatite metasomatism in the northern Tanzanian mantle: Petrographic and geochemical characteristics[J]. Earth and Planetary Science Letters, 114(4): 463−475.

Shu Liangshu, Zhou Xinmin. 2002. Late Mesozoic tectonism of Southeast China[J]. Geological Review, 48(3): 249− 260 (in Chinese with English abstract).

Smith Raymond E., Smith Sidney E.. 1976. Comments on the use of Ti, Zr, Y, Sr, K, P and Na in classification of basaltic magmas [J]. Earth and Planetary Science Letters, 32: 114−120.

Song Chuanzhong, Li Jiahao, Yan Jiayong, Wang Yangyang, Liu Zhendong, Yuan Fang, Li Zhenwei. 2019. A tentative discussion on some tectonic problems in the east of South China continent[J]. Geology in China, 46(4): 704− 722(in Chinese with English abstract).

Sun S S, McDonough William F. 1989. Chemical and isotopic systematics of oceanic basalts: Implications for mantle composition and processes[J]. Geological Society of London Special Publications, 42 (1): 313−345.

Tang Limei, Chen Hanlin, Dong Chuanwan, Shen Zhongyue, Cheng Xiaogan, Fu Lulu. 2010. Late Mesozoic extension in SE China: Evidence from the basic dike swarms in Hainan Island, China[J]. Acta Petrology Sinica, 26(4):1204−1216 (in Chinese with English abstract).

Wang Dezi, Shu Liangshu. 2012. Late Mesozoic basin and range tectonics and related magmatism in Southeast China[J]. Geoscience Frontiers, 3(2): 109−124.

Wang Dezi, Zhao Guangtao, Qiu Jiansheng. 1995. The tectonic constraint on the late mesozoic A− type granitoids in eastern China[J]. Geological Journal of Universities, 1(2):13− 21(in Chinese with English abstract).

Wang Diwen. 2013. 1∶25,000 Geological Survey Report of Yifeng[R]. Geological Survey of Jiangxi Province(in Chinese with English abstract).

Wang Guoguang, Ni Pei, Yao Jing, Wang Xiaolei, Zhao Kuidong, Zhu Renzhi, Xu Yingfeng, Pan Junyi, Li Li, Zhang Yinghong. 2015. The link between subduction− modified lithosphere and the giant Dexing porphyry copper deposit, South China: Constraints from high−Mg adakitic rocks[J]. Ore Geology Reviews, 67: 109−126.

Wang Guoguang, Ni Pei, Zhao Chao, Wang Xiaolei, Li Pengfei, Chen Hui, Zhu Andong, Li Li. 2006a. Spatiotemporal reconstruction of Late Mesozoic silicic large igneous province and related epithermal mineralization in South China: Insights from the Zhilingtou volcanic−intrusive complex [J]. Journal of Geophysical Research: Solid Earth, 121(11): 7903−7928.

Wang Qiang, Xu Jifeng, Jian Ping, Bao Zhiwei, Zhao Zhenhuan, Li Chaofeng, Xiong Xiaolin, Ma Jinlong. 2006b. Petrogenesis of adakitic porphyries in an extensional tectonic setting, dexing, South China: Implications for the genesis of porphyry copper mineralization [J]. Journal of Petrology, 47(1): 119−144.

Wang Qiang, Zhao Zhenhua, Jian Ping, Xiong Xiaolin, Bao Zhiwei, Dai Tongmo, Xu Jifeng, Ma Jinlong. 2005. Geochronology of Cretaceous A− type granitoids or alkaline intrusive rocks in the hinterland, South China: Constraints for Late− Mesozoic tectonic evolution[J]. Acta Petrologica Sinica, 21(3): 75− 808 (in Chinese with English abstract).

Wang Yuejun, Liao Chaolin, Fan Weiming, Peng Touping. 2004. Early Mesozoic OIB− type alkaline in central Jiangxi Province and its tectonic implications[J]. Geochimica, 33(2):109− 117 (in Chinese with English abstract).

Wang Yuejun, Fan Weiming, A.Cawood Peter, Li Sandzhong. 2008. Sr− Nd− Pb isotopic constraints on multiple mantle domains for Mesozoic mafic rocks beneath the South China Block hinterland[J]. Lithos, 106: 297−308.

Wang Yuejun, Fan Weiming, Zhang, Guowei, Zhang, Yanhua. 2013. Phanerozoic tectonics of the South China Block: Key observations and controversies[J]. Gondwana Research, 23(4): 1273−1305.

Wood David A. 1980. The application of a Th− Hf− Ta diagram to problems of tectomagmatic classification and establishing the nature of crustal contamination of basaltic lavas of the British Tertiary volcanic province[J]. Earth and Planetary Science Letters, 50: 11−30.

Xie Guiqing. 2003. Late Mesozoic and Cenozoic Mafic Dikes (bodies) from Southeastern China: Geological and Geochemical Characteristics and Its Geodynamics——A Case of Jiangxi Province[D]. Guiyang: Institute of Geochemistry Chinese Academy of Sciences, 2003 (in Chinese with English abstract).

Xu Xianbing, Tang Shuai, Li Yuan, Zhang Zejun. 2015. Characteristics of Neoproterozoic− Early Mesozoic multiphase orogenic activities of eastern Jiangnan Orogen[J]. Geology in China, 42(1): 33−50(in Chinese with English abstract).

Yan Jiayong, Lü Qintian, Luo Fan, Chen Anguo, Ye Gaofeng, Zhang Yongqian, Zhang Kun, Zhao Jinhua, ZhangChong, Liu Zhendong, Liu Yan. 2019. Where is Qinzhou−Hangzhou juncture belt? Evidence from integrated geophysical exploration[J]. Geology in China, 46 (4): 690−703(in Chinese with English abstract).

Yan Jun, An Yajun, Chen Jiangfeng. 2011. Isotopic characteristics of the Mesozoic to Cenozoic basic rocks from Eastern China: Character of magmatic source and deep processe[J]. Geological Review, 57(4): 532−540 (in Chinese with English abstract).

Yang Minggui, Huang Shuibao, Lou Fasheng, Tang Weixin, Mao Subin. 2009. Lithospheric structure and large− scale metallogenic process in Southeast China continental area[J]. Geology in China, 36(3): 528−543(in Chinese with English abstract).

Yang Minggui, Mei Yongwen. 1997. Characteristics of geology and metatllization in the Qinzhou− Hangzhou paleoplate juncture[J]. Geology and Mincral Resources of South China, 3: 52− 59 (in Chinese with English abstract).

Yu Xinqi, Wu Ganguo, Zhang Da, Di Yongjun, Zang Wenshuan, Zhang Xiangxin, Wang Qunfeng. 2005. Research progress on Mesozoic tectonic system transformation in Southeast China[J]. Progress in Natural Science, 15(10): 1167−1174(in Chinese with English abstract).

Zhang Bangtong, Chen Peirong, Kong Xinggong. 2002. Rb−Sr chronology of bimodal volcanic rocks of the Yutian Group in the Linjiang basin, southern Jiangxi[J]. Geology in China, 29(4): 351−354 (in Chinese with English abstract).

Zhang Chuanlin, Zhu Qingbo, Chen Xiangyan, Ye Haimin. 2016. Ordovician arc− related mafic intrusions in South China: Implications for plate subduction along the southeastern margin of South China in the Early Paleozoic[J]. Journal of Geology, 124(6): 743−767.

Zhang Chuanlin, Zou Haibo, Zhu Qingbo, Chen Xiangyan. 2015. Late Mesoproterozoic to Early Neoproterozoic ridge subduction along southern margin of the Jiangnan Orogen: New evidence from the Northeastern Jiangxi Ophiolite (NJO), South China[J]. Precambrian Research, 268: 1−15.

Zhang Guishan, Wen Hanjie, Li Shilei, Hu Ruizhong, Qiu Yuzhuo. 2009. Geochemical characteristics of bojite in northern Fujian Province and their Geodynamic significance[J]. Acta Mineralogica Sinica, 29(2): 243−252 (in Chinese with English abstract).

Zhang Guowei, Guo Anlin, Wang Yuejun, Li Sanzhong, Dong Yunpeng, Liu Shaofeng, He Dengfa, Cheng Shunyou, Lu Rujui, Yao Anping. 2013. Tectonics of South China continent and its implications[J]. Science China Earth Sciences, 56(11): 1804−1828.

Zhao Xilin, Liu Kai, Mao Jianren, Ye Haimin. 2012. Metallogenesis of two types of late Early Yanshanian granitoids in South China: Case studies of south Jiangxi and southwest Fujian[J]. Geology in China, 39(4): 871−886(in Chinese with English abstract).

Zheng Yongfei. 2012. Metamorphic chemical geodynamics in continental subduction zones[J]. Chemical Geology, 328(0): 5−48.

Zheng Yongfei, Xiao Wenjiao, Zhao Guochun. 2013. Introduction to tectonics of China[J]. Gondwana Research, 23: 1189−1206.

Zhou Jincheng, Chen Rong. 2001. Geochemistry of late Mesozoic interaction between crust and mantle in southeastern Fujian Province[J]. Geochimica, 30(6): 547−559 (in Chinese with English abstract).

Zhou Taofa, Fan Yu, Yuan Feng, Song Chuanzhong, Zhang Lejun, Qian Cunchao, Lu Sanming, David R C. 2010. Temporal− spatial framework of magmatic intrusions in Luzong volcanic basinin East China and their constrain to mineralizations[J]. Acta Petrologica Sinica, 26(9): 2694−2714 (in Chinese with English abstract).

Zhou Xinmin, Li Wuxian. 2000. Origin of Late Mesozoic igneous rocks in Southeastern China: Implications for lithosphere subduction and underplat ing of mafic magmas[J]. Tectonophysics, 326: 269−287.

Zhou Xinmin, Sun T, Shen Weizhou, Shu Liangshu, Niu Y L. 2006. Petrogenesis of Mesozoic granitoids and volcanic rocks in South China: A response to tectonic evolution[J]. Episodes, 29(1):26−33.

附中文参考文献

崔建军, 张岳桥, 董树文, 江博明, 徐先兵, 马立成, 李建军, 苏金宝, 李勇 . 2013. 华南陆缘晚中生代造山及其地质意义[J]. 中国地质, 40(1): 86−105.

董传万, 闫强, 张登荣, 杜振永, 竺国强 . 2010. 浙闽沿海晚中生代伸展构造的岩石学标志:东极岛镁铁质岩墙群[J]. 岩石学报, 26(4): 1195−1203.

范蔚茗,王岳军,郭锋, 彭头平 . 2003. 湘赣地区中生代铁镁质岩浆作用与岩石圈伸展[J]. 地学前缘, 10(3): 159−169.

葛肖虹, 刘俊来, 任收麦, 袁四化 . 2014. 中国东部中—新生代大陆构造的形成与演化[J]. 中国地质, 41(1): 19−38.

耿建珍,李怀坤,张健, 周红英, 李惠民 . 2011. 锆石Hf同位素组成的LA−MC−ICPMS测定[J]. 地质通报, 30(10): 1508−1513.

计波,黄博涛,李向民,王磊 . 2019.南祁连西北缘肃北红庙沟地区早奥陶世花岗岩年代学、地球化学特征及其地质意义[J]. 西北地质, 52(4):63−75.

江西省地质矿产局 . 1984. 江西省区域地质志[M]. 北京: 地质出版社 .

江西省地质矿产勘查开发局 . 2015. 江西省区域地质志[M]. 北京: 地质出版社 .

赖新平 . 1989. 江西新余1∶5万地质图及说明书[R]. 南昌: 江西省地

质矿产勘查开发局.
毛建仁, 厉子龙, 叶海敏. 2014. 华南中生代构造-岩浆活动研究: 现状与前景[J]. 中国科学: 地球科学, 44: 2593-2617.
毛景文, 陈懋弘, 袁顺达, 郭春丽. 2011. 华南地区钦杭成矿带地质特征和矿床时空分布规律[J]. 地质学报, 85(5): 636-658.
毛景文, 李红艳,王登红. 1998. 华南地区中生代多金属矿床形成与地幔柱关系[J]. 矿物岩石地球化学通报, 19(2):130-132.
倪培, 王国光. 2017. 大陆再造与钦杭带北东段多期铜金成矿作用[J]. 岩石学报, 33(11): 3373-3394.
彭戈, 延峻, 初晓强, 李全忠, 陈志洪. 2012. 贵池岩体锆石定年和地球化学:岩石成因和深部过程[J]. 岩石学报, 28(10): 3271-3286.
齐有强, 胡瑞忠, 刘燊, 戚华文, 冯彩霞. 2008. 赣杭构造带中西段中生代基性脉岩地球化学特征[J]. 吉林大学学报(地球科学版), 38(5): 784-794.
秦社彩, 范蔚茗, 郭锋, 李超文, 高晓峰. 2007. 浙闽晚中生代辉绿岩脉的岩石成因:年代学与地球化学制约[J]. 岩石学报, 26(11): 3295-3306.
宋传中, 李加好, 严加永, 王阳阳, 刘振东, 袁芳, 李振伟. 2019. 华南大陆东部若干构造问题的思考[J]. 中国地质, 46(4): 704-722.
舒良树, 周新民. 2002. 中国东南部晚中生代构造作用[J]. 地质论评, 48(3): 249-260.
唐立梅, 陈汉林, 董传万, 沈忠悦, 程晓敢, 付璐露. 2010. 中国东南部晚中生代构造伸展作用——来自海南岛基性岩墙群的证据[J]. 岩石学报, 26(4): 1204-1216.
王德滋, 赵广涛, 邱检生. 1995. 中国东部晚中生代A型花岗岩的构造制约[J]. 高校地质学报, 1(2): 13-21.
王迪文. 2013. 1:25万宜春幅区域地质调查报告[R].江西省地质调查研究院.
王岳军, 廖超林, 范蔚茗, 彭头平. 2004. 赣中地区早中生代OIB碱性玄武岩的厘定及构造意义[J]. 地球化学, 33(2): 109-117.
谢桂青. 2003. 中国东南部晚中生代以来的基性岩脉(体)的地质地球化学特征及其地球动力学意义初探———以江西省为例[D]. 贵阳:中国科学院地球化学研究所.
徐先兵, 汤帅, 李源, 章泽军. 2015. 江南造山带东段新元古代至早中生代多期造山作用特征[J]. 中国地质, 42(1): 33-50.
严加永,吕庆田,罗凡,陈安国,叶高峰,张永谦,张昆,赵金花,张冲,刘振东,刘彦. 2019. 钦杭何在？来自综合地球物理探测的认识[J]. 中国地质, 46(4): 690-703.
闫峻, 安亚军, 陈江峰. 2011. 中国东部中—新生代基性岩的同位素特征:源区性质及深部过程[J]. 地质论评, 57(4): 532-540.
杨明桂, 梅勇文. 1997. 钦—杭古板块结合带与成矿带的主要特征[J]. 华南地质与矿产, 3: 52-59.
杨明桂, 黄水保, 楼法生, 唐维新, 毛素斌. 2009. 中国东南陆区岩石圈结构与大规模成矿作用[J]. 中国地质, 36(3): 528-543.
余心起, 吴淦国, 张达, 狄永军, 臧文拴, 张祥信, 汪群峰. 2005. 中国东南部中生代构造体制转换作用研究进展[J]. 自然科学进展, 15(10): 1167-1174.
章邦桐,陈培荣,孔兴功.2002. 赣南临江盆地余田群双峰式火山岩的Rb-Sr年代学研究[J]. 中国地质, 29(4): 351-354.
张贵山, 温汉捷, 李石磊, 胡瑞忠, 裘愉卓. 2009. 闽北角闪辉长岩的地球化学特征及其地球动力学意义[J]. 矿物学报, 29(2): 243-252.
赵希林, 刘凯, 毛建仁, 叶海敏. 2012. 华南燕山早期晚阶段两类花岗质岩体与成矿作用: 以赣南—闽西南地区为例[J]. 中国地质, 39(4): 871-886.
周金城, 陈荣. 2001. 闽东南晚中生代壳幔作用地球化学[J]. 地球化学, 30(6): 547-559.
周涛发, 范裕,袁峰, 宋传中, 张乐骏, 钱存超, 陆三明, David R C. 2010. 庐枞盆地侵入岩的时空格架及其对成矿的制约[J]. 岩石学报, 26(9): 2694-2714.